

基于 2-甲基-8-羟基喹啉的镝单分子磁体的晶体结构及磁性

王慧娜 刘颖昕 李 荣 周 琦* 付文升*

(重庆师范大学, 重庆市绿色合成与应用重点实验室, 重庆 401331)

摘要: 以 2-甲基-8-羟基喹啉(HL)为配体合成了 2 个含有镝离子的配位化合物 $[\text{Dy}_2\text{L}_4(\text{HL})_4(\text{H}_2\text{O})_2](\text{ClO}_4)_2 \cdot 2\text{H}_2\text{O}$ (**1**)和 $[\text{Dy}_2\text{L}_6(\text{C}_2\text{H}_5\text{OH})] \cdot \text{H}_2\text{O}$ (**2**)。虽然在这两个配位化合物中配体都是 2-甲基-8-羟基喹啉,但其参与配位的方式不同。这导致 2 个化合物中镝离子所处的配位环境不同,进而对化合物的磁性产生了影响。

关键词: 配位化合物; 分子磁体; 镧系金属; 磁弛豫作用

中图分类号: O614.342 文献标识码: A 文章编号: 1001-4861(2016)02-0343-08

DOI: 10.11862/CJIC.2016.047

Structures and Magnetic Properties of Single-Molecule Magnet Based on Dy(III) and 2-Methyl-8-quinolinol Ligand

WANG Hui-Na LIU Ying-Xin LI Rong ZHOU Qi* FU Wen-Sheng*

(Chongqing Key Laboratory of Green Synthesis and Applications, Chongqing Normal University, Chongqing 401331, China)

Abstract: Two dysprosium coordination compounds, $[\text{Dy}_2\text{L}_4(\text{HL})_4(\text{H}_2\text{O})_2](\text{ClO}_4)_2 \cdot 2\text{H}_2\text{O}$ (**1**) and $[\text{Dy}_2\text{L}_6(\text{C}_2\text{H}_5\text{OH})] \cdot \text{H}_2\text{O}$ (**2**), have been synthesized and characterized. Both compounds contain the same ligands 2-methyl-8-hydroxyl-quinolinol (HL), while the different coordination modes lead to quite different coordination environments. Magnetic measurements reveal that the different coordination modes of the ligand lead to a difference in the dynamic magnetic behaviors. Compound **1** does show a single-molecule magnet behavior, while no out-of-phase signals are observed in compound **2**. CCDC: 1054513, **1**; 1052697, **2**.

Keywords: coordination compound; molecule magnet; lanthanide metal; magnetic relaxation

Over the past decade, single-molecule magnet (SMM) has received considerable attention due to potential applications in high density data storage and quantum computer^[1-5]. The early research of single-molecule magnet mainly focused on 3d transition metal clusters, especially on Mn element. A considerable amount of Mn clusters with various structures has been synthesized, such as $[\text{Mn}_{32}]$, $[\text{Mn}_{84}]$ ^[6-10]. Besides, their magnetic properties have been studied extensively. Although 3d transition metal clusters have high ground state spins, the feeble magnetic anisotropy

limits further increase energy barrier of SMM^[11-12]. Thus, 4f lanthanide ion with strong magnetic anisotropy is introduced into 3d transition metal clusters in order to form 3d-4f heteronuclear metal clusters that may combine the large magnetic anisotropy of lanthanide ions with the high spin-states of transition ions^[13-17]. In recent years, design and synthesis of 4f compounds which only contain lanthanide metal have become the topic on single-molecule magnet research, and a number of lanthanide metal clusters have been synthesized, such as $[\text{Th}_2]$, $[\text{Dy}_2]$, $[\text{Dy}_3]$, $[\text{Dy}_4]$, $[\text{Dy}_5]$,

收稿日期: 2015-09-09。收修改稿日期: 2015-12-30。

国家自然科学基金(No.21271192, 21501017)、重庆市教委科学技术研究项目(No.KJ1500304)和重庆市科委国际合作项目(No.cstc2014gjh0030)资助。

*通信联系人。E-mail: fuwensheng@hotmail.com, lnwoq172@163.com; 会员登记号: S06N0386S1202。

[Dy₆]^[18-23]. These compounds could play a significant role in SMM area owing to their large magnetic moments and huge magnetic anisotropy. This combination may lead to a high barrier for their spin reversal.

It has been demonstrated that the overall electronic structure of lanthanide ion is very sensitive to its coordination environment. Even subtle ligand changes can drastically influence on the overall physical properties of the lanthanide compounds, and the SMM behaviour of lanthanide ions is highly dependent on the ligands^[24-31]. We also investigated the effect of different ligands on the magnetic exchange interactions and the relaxation dynamics^[32-33]. As we noticed that the same ligand could lead to different coordination environment, we wonder what will happen in the compounds contain the same ligands. For example, 2-methyl-8-hydroxyquinolate (HL) can coordinate to metal ions with two modes, chelating or not. It will certainly lead to a quite different coordination environment (coordination numbers and geometries), and in turn, it may make a difference in the magnetic behaviours.

In this paper, we synthesized two dysprosium coordination compounds with binuclear structure using HL as ligand, namely [Dy₂L₄(HL)₄(H₂O)₂](ClO₄)₂·2H₂O (**1**) and [Dy₂L₆(C₂H₅OH)]·H₂O (**2**). As we anticipated, the coordination environment of the Dy³⁺ ions was significantly different. The Dy³⁺ ion in both of the compounds is eight-coordinated. In compound **1**, the dinuclear core is bridged by two O ions, giving rise to a [Dy₂O₂] core. In compound **2**, the two Dy ions are bridged by three O ions, which form a [Dy₂O₃] core. Magnetic measurements demonstrate that the compounds exhibit weak intra-binuclear antiferromagnetic interaction. Compound **1** show frequency-dependent ac-susceptibility indicative of slow magnetic relaxation. On the contrary, no out-of-phase ac susceptibility (χ'') signal was observed in **2**.

1 Experimental

1.1 Reagents and physical measurements

All reagents and solvents were commercially

available and were used without further purification. Elemental analyses of carbon and hydrogen were carried out on a Perkin-Elmer 240C elemental analyzer. IR spectra as KBr pellets were recorded with a Magna 750 FT-IR spectrophotometer using reflectance technique over the range of 4 000~400 cm⁻¹. X-ray powder diffraction (XRPD) patterns were taken on a Rigaku D/max 2550 X-ray Powder Diffractometer with Cu K α radiation ($\lambda=0.154\ 18\ \text{nm}$, $U=30\ \text{kV}$, $I=40\ \text{mA}$). All magnetization were obtained with a Quantum Design MPMS SQUID VSM magnetometer. The variable-temperature magnetic susceptibility was measured with an external magnetic field of 1 000 Oe. Samples were restrained in eicosane to prevent torqueing. Pascal's constants were used to estimate the diamagnetic corrections, which were subtracted from the experimental susceptibilities to give the molar paramagnetic susceptibilities (χ_M).

1.2 Synthesis

[Dy₂L₄(HL)₄(H₂O)₂](ClO₄)₂·2H₂O (**1**): A mixture of Dy(ClO₄)₃·6H₂O (0.25 mmol, 0.14 g) and HL (1.0 mmol, 0.159 g) in a mixture of ethanol (8 mL) and acetonitrile (2 mL) was stirred for 30 min, then the resulting mixture were filtered. The filtrate was heated at 60 °C for 7 days in a Teflon-lined steel autoclave (20 mL). Yellow block-shaped crystals formed and were collected in 40% yield. IR (KBr, cm⁻¹): 3 233(m), 3 178(m), 3 061(w), 1 645(m), 1 586(s), 1 454(s), 1 432(m), 1 348(s), 1 121(m), 1 001(w), 935(m), 855(m), 813(s), 716(m), 576(m). Anal. Calcd. for C₈₀H₇₆N₈Cl₂Dy₂O₂₀(%): C 51.51, H 4.11, N 6.01. Found(%): C, 51.28, H 4.09, N 5.91.

[Dy₂L₆(C₂H₅OH)]·H₂O (**2**): A mixture of Dy(ClO₄)₃·6H₂O (0.25 mmol, 0.14 g) and HL (0.75 mmol, 0.119 g) in ethanol (10 mL) was stirred for 30 min, then the resulting mixture were filtered. The filtrate was heated at 80 °C for 3 days in a Teflon-lined steel autoclave (20 mL). Yellow block-shaped crystals formed were collected in 37% yield. IR (KBr, cm⁻¹): 3 245(m), 3 089(w), 3 061(w), 1 606(m), 1 569(s), 1 494(s), 1 465(s), 1 381(s), 1 118(s), 1 024(m), 911(w), 826(m), 816(s), 733(m), 489(m). Anal. Calcd. for C₆₂H₅₆N₆Dy₂O₈(%): C 55.65, H 4.22, N 6.28. Found (%): C, 55.38, H 4.15, N 6.22.

1.3 X-ray crystallography

The data collection and structural analysis of crystals **1** and **2** were performed on a Rigaku RAXIS-RAPID equipped with a narrow-focus, 5.4 kW sealed tube X-ray source (graphite-monochromated Mo $K\alpha$ radiation, $\lambda=0.071\ 073$ nm). The data processing was accomplished with the PROCESS-AUTO processing program. The data were collected at a temperature of 293(2) K. Direct methods were used to solve the

structure using the SHELXTL crystallographic software package^[34]. All non-hydrogen atoms were easily found from the difference Fourier map. All non-hydrogen atoms were refined anisotropically. The hydrogen atoms were set in calculated positions. Crystal data for compounds are listed in Table 1, and selected bond lengths and angles for compounds are listed in Table 2 and Table 3.

CCDC: 1054513, **1**; 1052697, **2**.

Table 1 Crystallographic data for the compounds **1** and **2**

Compound	1	2
Empirical formula	C ₈₀ H ₇₆ N ₈ Cl ₂ Dy ₂ O ₂₀	C ₆₂ H ₅₆ N ₆ Dy ₂ O ₈
Formula weight	1 865.39	1 338.13
Crystal system	Monoclinic	Triclinic
Space group	$P2_1/c$	$P\bar{1}$
a / nm	1.243 5(3)	1.363 7(3)
b / nm	2.212 3(4)	1.442 5(3)
c / nm	1.761 9(6)	1.557 8(3)
α / (°)	90	94.14(3)
β / (°)	128.51(2)	98.47(3)
γ / (°)	90	104.43(3)
V / nm ³	3.792 8(17)	2.916 2(10)
Z	2	2
D_c / (g·cm ⁻³)	1.633	1.524
μ / mm ⁻¹	2.106	2.601
$F(000)$	1 876	1 332
θ range for all data collection / (°)	6.81~26.00	3.08~26.00
Reflections collected	31 991	24 991
Unique reflections	7 312	11 229
R_{int}	0.110 8	0.029 4
Goodness-of-fit on F^2	1.057	1.081
R_1^a [$I > 2\sigma(I)$]	0.067 5	0.036 8
wR_2^b [$I > 2\sigma(I)$]	0.153 4	0.111 9
R_1^a (all data)	0.115 2	0.043 3
wR_2^b (all data)	0.117 33	0.123 1

$$^a R_1 = \sum \|F_o\| - \|F_c\| / \sum \|F_o\|; ^b wR_2 = \{ \sum [w(F_o^2 - F_c^2)^2] / \sum [w(F_o^2)]^2 \}^{1/2}; w = 1 / [\sigma^2(F_o^2) + (0.051 - 1P)^2 + 19.56P], \text{ where } P = [|F_o|^2 + 2|F_c|^2] / 3.$$

Table 2 Main bond lengths (nm) and angles (°) of compound **1**

Dy1-O4	0.223 9(5)	Dy1-O2	0.227 6(5)	Dy1-O1	0.234 7(4)
Dy1-O1#	0.250 4(5)	Dy1-O3	0.227 9(4)	Dy1-O5	0.267 5(5)
Dy1-N3	0.270 7(5)	Dy1-N2	0.273 0(6)	Dy1...Dy1A	0.404 3(1)
Dy1-O1-Dy1A	112.9(2)				

Symmetry code: A: $-x, -y-1, -z+1$

Table 3 Main bond lengths (nm) and angles (°) of compound **2**

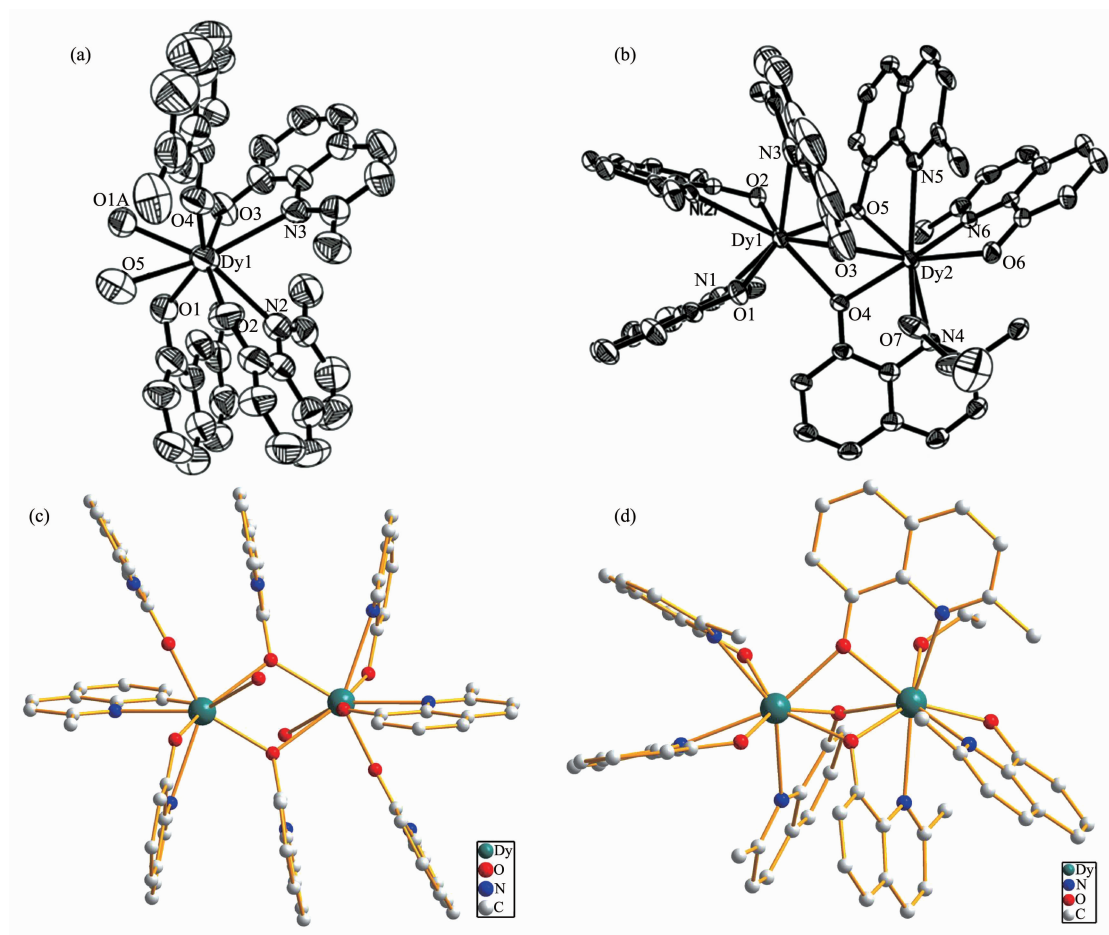
Dy1-O2	0.221 6(4)	Dy1-O1	0.226 9(4)	Dy1-O3	0.234 4(4)
Dy1-O4	0.238 6(4)	Dy1-O5	0.236 4(3)	Dy1-N2	0.262 8(4)
Dy1-N3	0.266 0(5)	Dy1-N1	0.260 1(5)	Dy2-O6	0.222 1(4)
Dy2-O5	0.230 2(3)	Dy2-O3	0.235 4(4)	Dy2-O4	0.235 7(4)
Dy2-O7	0.237 9(4)	Dy2-N6	0.260 0(5)	Dy2-N5	0.261 2(4)
Dy2-N4	0.264 6(4)	Dy1...Dy2	0.351 2(1)		
Dy1-O3-Dy2	96.84(15)	Dy1-O4-Dy2	95.58(13)	Dy1-O5-Dy2	97.66(13)

2 Results and discussion

2.1 Crystal structure

Compound **1** crystallizes in the monoclinic space group $P2_1/c$ and the structure is shown in Fig.1a. The dysprosium ion is coordinated by two bridging ligand (O1, O1A), two chelating ligand (O2, N2, O3, N3),

one terminal ligand (O4) and one water molecules (O5). The eight-coordinated Dy ions are characterized by distorted biaugmented trigonal prism geometry, as calculated using the SHAPE software. Besides, there is one isolated water molecule and one perchlorate which is the counterion in the asymmetric structure unit. The centrosymmetric dinuclear core is composed



Hydrogen atoms and minor disordered components have been omitted for clarity; Thermal ellipsoids are drawn at 50% probability in (a) and (b); Symmetry code: A: $-x, -y-1, -z+1$ for **1**

Fig.1 (a) Coordination environment of Dy(III) ion in compound **1**; (b) Coordination environments of Dy(III) ions in compound **2**; (c) Molecular structure of compound **1**; (d) Molecular structure of compound **2**

of two eight coordinate dysprosium ions bridged by two ions bridged by two oxygen ions, giving rise to a Dy_2O_2 core with a Dy-Dy distance of 0.404 3(1) nm and a Dy-O-Dy angle of $113.9(2)^\circ$. Similar Ln_2O_2 structures have been also reported, such as $[\text{Dy}_2(\text{hmi})_2(\text{NO}_3)_2(\text{MeOH})_2]$, $[\text{Dy}_2(\text{ovph})_2(\text{NO}_3)_2(\text{H}_2\text{O})_2]$, $[\text{Tb}_2(\text{valdien})_2(\text{NO}_3)_2]$ and $[\text{Gd}_2(\text{Hsabhea})_2(\text{NO}_3)_2]$ ^[26,31,37]. The shortest intermolecular Dy-Dy separation distance is 1.139 7(5) nm. Only two HL molecules coordinate to metal ions with a chelating mode, and the rest were not.

Compound **2** crystallizes in the triclinic space group $P\bar{1}$ and the structure is shown in Fig.1b. The Dy^{3+} ions are eight-coordinated and characterized by a triangular dodecahedron environment (calculated by means of SHAPE software). Dy1 is coordinated by three chelating ligands (O1, O2, O3, N1, N2 and N3) and two bridging oxygen atoms (O4 and O5). Dy2 is coordinated by three chelating ligands (O4, O5, O6, N4, N5 and N6), one bridging oxygen atoms (O3), and one terminal ethanol (O7). Two eight coordinate dysprosium ions are bridged by three oxygen atoms, giving rise to a Dy_2O_3 core with a Dy-Dy distance of 0.351 2(1) nm. The Dy-O-Dy angles are $96.84(15)^\circ$, $95.58(13)^\circ$ and $97.33(13)^\circ$, respectively. The shortest intermolecular Dy-Dy separation distance is 0.866 9(5) nm. In contrast with compound **1**, all the ligands coordinating to Dy^{3+} ions have a chelating mode.

Although both of **1** and **2** contain two eight coordinate dysprosium ions, the coordination environments of Dy^{3+} ions are different. In compound **1**, the Dy^{3+} ions are characterized by a distorted dodecahedral environment, and the Dy_2O_2 core is centrosymmetric. On the other hand, in compound **2**, the Dy^{3+} ions are characterized by a square antiprism environment, and the Dy_2O_3 core is non-centrosymmetric. We expected that the differences of coordination environments could influence on the magnetic properties of the compounds.

2.2 Magnetic properties

The solid-state variable-temperature direct-current (dc) magnetic susceptibility measured for the compounds have been carried out in an applied

magnetic field of 1 000 Oe in the temperature range of 2~300 K. The plots of $\chi_{\text{M}}T$ vs T are shown in Fig.2. For compounds **1** and **2**, the room temperature $\chi_{\text{M}}T$ values are 27.98 and 27.46 $\text{cm}^3 \cdot \text{K} \cdot \text{mol}^{-1}$, respectively, in good agreement with that expected for two uncoupled Dy ions ($^6H_{15/2}$, $S=5/2$, $L=5$, $J=15/2$, $g=4/3$, $\chi_{\text{M}}T=14.17 \text{ cm}^3 \cdot \text{K} \cdot \text{mol}^{-1}$). Upon decreasing the temperature, the $\chi_{\text{M}}T$ slightly decreases between 300 K and 25 K, then further decreases sharply until reaches values of 11.28 and 13.45 $\text{cm}^3 \cdot \text{K} \cdot \text{mol}^{-1}$ at 2 K, respectively. The overall behaviours of $\chi_{\text{M}}T$ are caused by thermal depopulation of the Stark sublevels and significant magnetic anisotropy of the dysprosium ions. The weak antiferromagnetic interactions between the metal centres may also make some contribution^[35].

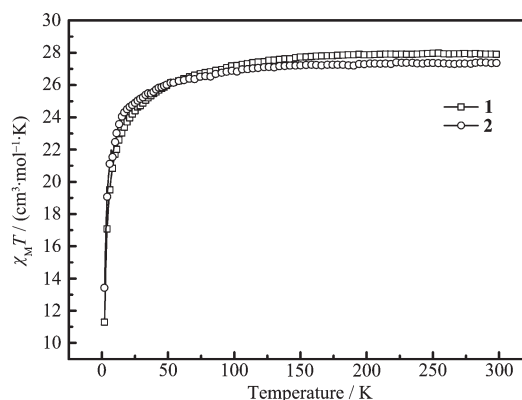


Fig.2 Temperature dependence of $\chi_{\text{M}}T$ for compounds **1** and **2** at 1 000 Oe

Field-dependence measurements of the magnetization up to 5 T were performed at 2 K. For compounds **1** and **2**, the values of the magnetization at 5 T are $10.59\mu_{\text{B}}$ and $10.22\mu_{\text{B}}$, respectively, lower than the expected saturation value of $20\mu_{\text{B}}$ for two Dy ions. The spin orbit coupling and crystal-field effect may make the contributions^[36]. The lack of saturation on the M vs H data confirms low lying excited states.

To further investigate magnetization dynamics of the compounds, alternating-current (ac) susceptibility measurements have been carried out (dc field 0 Oe, ac field 3.0 Oe, frequency 10~800 Hz). As shown in Fig.3, frequency-dependent on alternating-current magnetic susceptibilities are observed in compound **1**. This indicates the presence of slow magnetic relaxation at low temperature, which reveals the

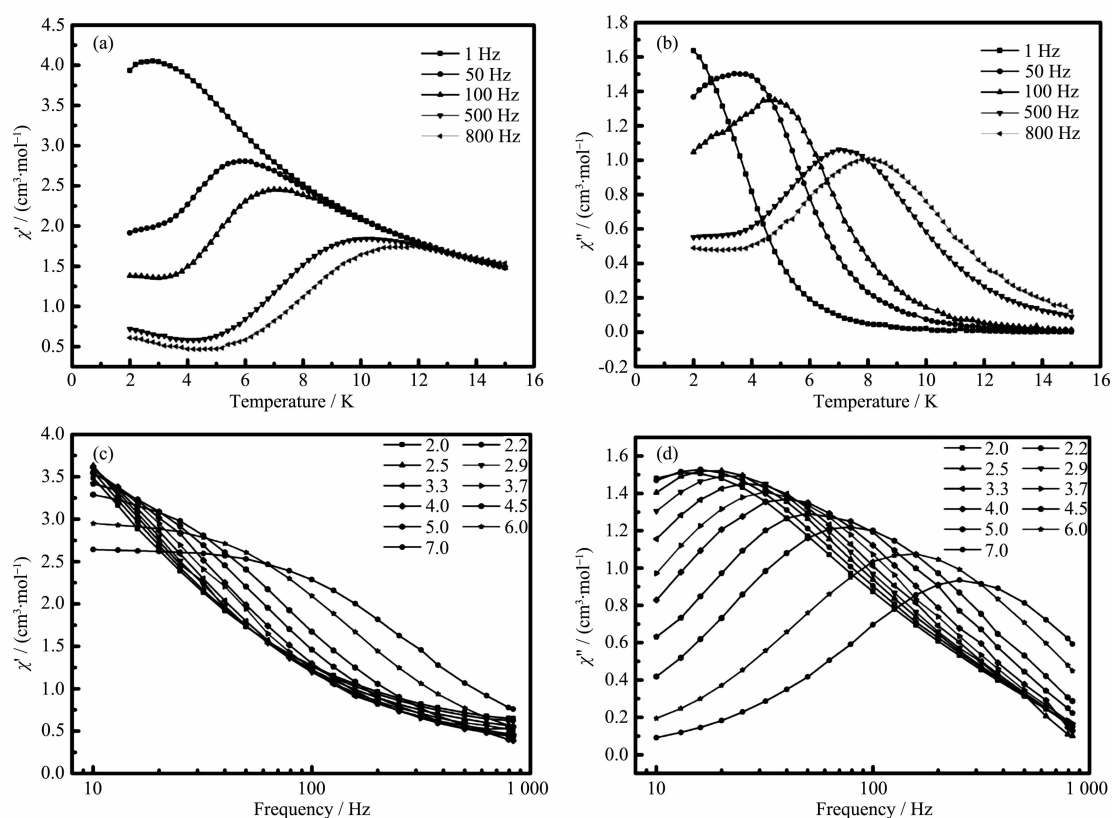
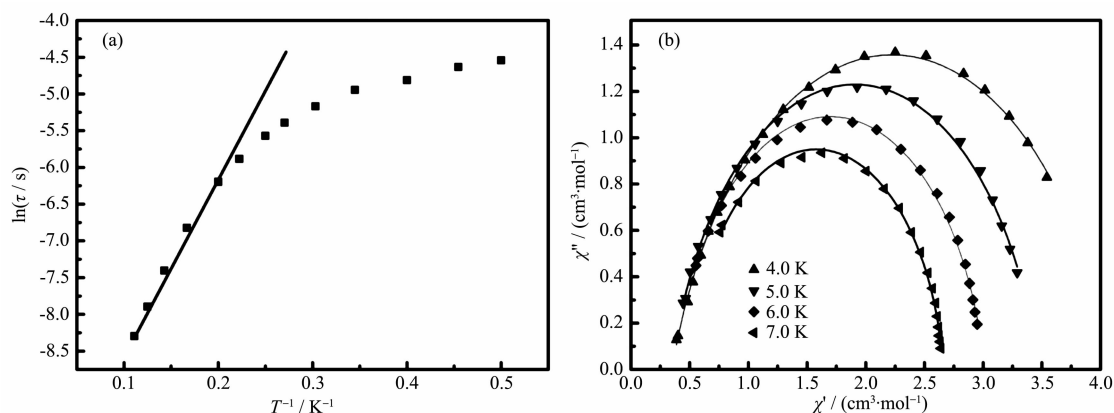


Fig.3 Temperature dependence of the in-phase (a) and out-of-phase (b) ac susceptibility and frequency dependence of in-phase (c) and out-of-phase (d) ac susceptibilities for compound **1** under zero dc field

single-molecule magnet behavior.

The relaxation time was extracted from the frequency-dependent data, and the Arrhenius plot obtained from these data is showed in Fig.4a. The relaxation follows a thermally activated mechanism with an energy barrier of 17.2 K and a pre-exponential factor of $\tau_0 = 5.91 \times 10^{-5}$ s, in agreement with that for Dy^{III} single-molecule magnet with binuclear

structure ($\Delta E/k_B$ 17~198 K, τ_0 10^{-8} ~ 10^{-5} s)^[37-38]. The data plotted as Cole-Cole plots can be fitted to the generalized Debye model with α parameters below 0.20 (Fig.3b), indicating the presence of a single relaxation process^[39-40]. On the contrary, no out-of-phase signals were observed in compound **2** (Fig.5). Thus, it may be inferred that the different coordination modes of the ligand can drastically influence on the



Solid line is fitted with Arrhenius law in (a) and the best fit obtained with a generalized Debye model in (b)

Fig.4 (a) $\ln(\tau)$ versus T^{-1} plot for compound **1** under zero dc field; (b) Cole-Cole plots measured for compound **1**

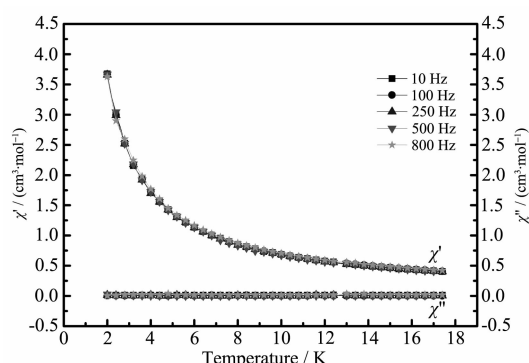


Fig.5 Temperature dependence of the in-phase and out-of-phase ac susceptibility for **2** under zero dc field

dynamic magnetic behaviors of the lanthanide compounds.

3 Conclusions

In summary, we have synthesized two dysprosium coordination compounds, $[\text{Dy}_2\text{L}_4(\text{HL})_4(\text{H}_2\text{O})_2](\text{ClO}_4)_2 \cdot 2\text{H}_2\text{O}$ (**1**) and $[\text{Dy}_2\text{L}_6(\text{C}_2\text{H}_5\text{OH})]\cdot\text{H}_2\text{O}$ (**2**) with the same ligands HL. Magnetic measurements reveal that compound **1** does show a single-molecule magnet behavior with the energy barrier $\Delta E/k_B = 17.1$ K and the pre-exponential factor $\tau_0 = 5.95 \times 10^{-5}$ s, while no out-of-phase signals are observed in compound **2**. It may be inferred that the different coordination modes of the ligand lead to a difference in the dynamic magnetic behaviors of the lanthanide coordination compounds.

Supporting information is available at <http://www.wjhxxb.cn>

References:

- [1] Leuenberger M N, Loss D. *Nature*, **2001**,**410**:789-791
- [2] Hill S, Edwards R S, Aliaga-Alcalde N, et al. *Science*, **2003**,**302**:1015-1018
- [3] Yamanouchi M, Chiba D, Matsukura F, et al. *Nature*, **2004**,**428**:539-542
- [4] Saitoh E, Miyajima H, Yamaoka T, et al. *Nature*, **2004**,**432**:203-206
- [5] Bogani L, Wernsdorfer W. *Nat. Mater.*, **2008**,**7**:179-186
- [6] Maheswaran S, Chastanet G, Teat S J, et al. *Angew. Chem. Int. Ed.*, **2004**,**43**:2117-2121
- [7] Scott R T W, Milios C J, Vinslava A, et al. *Dalton Trans.*, **2006**:3161-3163
- [8] Wang W G, Zhou A J, Zhang W X, et al. *J. Am. Chem. Soc.*, **2007**,**129**:1014-1015
- [9] Stamatatos T C, Foguet-Albiol D, Wernsdorfer W, et al. *Chem. Commun.*, **2011**,**47**:274-276
- [10] Ako A M, Hewitt I J, Mereacre V, et al. *Angew. Chem. Int. Ed.*, **2006**,**45**:4926-4929
- [11] Milios C J, Vinslava A, Wood P A, et al. *J. Am. Chem. Soc.*, **2007**,**129**:8-9
- [12] Milios C J, Vinslava A, Wernsdorfer W, et al. *J. Am. Chem. Soc.*, **2007**,**129**:2754-2755
- [13] Benelli C, Gatteschi C. *Chem. Rev.*, **2002**,**102**:2369-2387
- [14] Osa S, Kido T, Matsumoto N, et al. *J. Am. Chem. Soc.*, **2004**,**126**:420-421
- [15] Kong X J, Ren Y P, Long L S, et al. *J. Am. Chem. Soc.*, **2007**,**129**:7016-7017
- [16] Mereacre V M, Ako A M, Clérac R, et al. *J. Am. Chem. Soc.*, **2007**,**129**:9248-9249
- [17] Ako A M, Mereacre V, Clérac R, et al. *Chem. Commun.*, **2009**,**45**:544-546
- [18] Yue Y, Sun J, Yan P, et al. *Inorg. Chem. Commun.*, **2015**,**51**:42-45
- [19] Hewitt I J, Lan Y, Anson C E, et al. *Chem. Commun.*, **2009**,**45**:6765-6767
- [20] Lin P H, Burchell T J, Ungur L, et al. *Angew. Chem. Int. Ed.*, **2009**,**48**:9489-9492
- [21] Blagg R J, Muryn C A, McInnes E J, et al. *Angew. Chem. Int. Ed.*, **2011**,**50**:6530-6533
- [22] Rinehart J D, Fang M, Evans W J, et al. *Nat. Chem.*, **2011**,**3**:538-542
- [23] Rinehart J D, Fang M, Evans W J, et al. *J. Am. Chem. Soc.*, **2011**,**133**:14236-14269
- [24] Sessoli R, Powell A K. *Coord. Chem. Rev.*, **2009**,**253**:2328-2341
- [25] Long J, Habib F, Lin P H, et al. *J. Am. Chem. Soc.*, **2011**,**133**:5319-5328
- [26] Ke H., Xu G F, Guo Y N, et al. *Chem. Commun.*, **2010**,**46**:6057-6059
- [27] Tian H, Wang M, Zhao L, et al. *Chem. Eur. J.*, **2012**,**18**:442-445
- [28] Ma Y, Xu G F, Yang X, et al. *Chem. Commun.*, **2010**,**46**:8264-8266
- [29] Guo Y N, Xu G F, Wernsdorfer W, et al. *J. Am. Chem. Soc.*, **2011**,**133**:11948-11951
- [30] Xu G F, Wang Q L, Gamez P, et al. *Chem. Commun.*, **2010**,**46**:1506-1508
- [31] Pointillart F, Klementieva S, Kuropatov V, et al. *Chem. Commun.*, **2012**,**48**:714-716
- [32] Yang F, Zhou Q, Zeng G, et al. *Dalton Trans.*, **2014**,**43**:

- 1238-1245
- [33]Zhou Q, Yang F, Liu D, et al. *Inorg. Chem.*, **2012**,**51**:7529-7536
- [34]Sheldrick G M. *SADABS, Siemens Area Detector Absorption Correction*, University of Göttingen, Germany, **2005**.
- [35]Kahn M L, Ballou R, Porcher P, et al. *Chem. Eur. J.*, **2002**, **8**:525-531
- [36]Osa S, Kido T, Matsumoto N, et al. *J. Am. Chem. Soc.*, **2004**,**126**:420-421
- [37]Song Y M, Luo F, Luo M B, et al. *Chem. Commun.*, **2012**, **48**:1006-1008
- [38]Zou L, Zhao L, Chen P, et al. *Dalton Trans.*, **2012**,**41**:2966-2971
- [39]Aubin S M J, Sun Z, Pardi L, et al. *Inorg. Chem.*, **1999**,**38**: 5329-5340
- [40]Cole K S, Cole R H. *J. Chem. Phys.*, **1941**,**9**:341-351